

## Supercurrents and dynamic resistivities in periodic arrays of superconducting-normal contacts\*

J. M. Dupart, J. Rosenblatt<sup>†</sup> and J. Baixeras  
*Laboratoire de Génie Electrique des Universités Paris VI et XI,<sup>‡</sup>*  
 33 Avenue du Général-Leclerc, 92260-Fontenay-aux-Roses, France  
 (Received 2 June 1977)

Periodic *SNSN* systems have been obtained by directional solidification of Pb-Sn lamellar eutectic. The temperature and field dependence of critical currents have been measured. The former is well described by a model of quantized quasiparticle levels in the normal regions. Supercurrents show interference patterns in the presence of a magnetic field which become less marked as the superconducting critical temperature of *Sn* is approached. An unexpected change of a few orders of magnitude in differential resistivity above the critical current is observed at a certain temperature in exceptionally clean samples. An attempt to explain this phenomenon is given in terms of the aforementioned quantized-level model.

### I. INTRODUCTION

After Josephson's prediction of the coupling of two superconductors by tunneling of Cooper pairs across an insulator, much work has been devoted to superconductor-insulator-superconductor (*S-I-S*) systems. Attention has also been directed towards another type of weak link in which the superconductors are coupled through a normal-metal layer or a region of weaker superconductivity as in Dayem bridges. In the present paper we are mainly interested in the behavior of superconductor-normal-metal-superconductor (*S-N-S*) or *S-S'-S* (*S'* is a superconductor different from *S*) systems formed by two different materials in a good metallurgical contact. This alternated structure is usually achieved by successive evaporations of the two components<sup>1,2</sup>; techniques of photolithography are also used in order to obtain series arrays of such junctions.<sup>3</sup> We have performed experiments on series arrays of *S-N-S* bridges obtained by directional solidification of lamellar eutectic alloys Pb-Sn.<sup>4</sup>

The first theory devoted to the *S-N-S* bridges is that of de Gennes,<sup>5</sup> which is valid when the two metals are in the dirty limit. Up to now most of the reported experimental results on evaporated systems have been explained in the framework of this theory even in the case where the mean free paths in the normal metal and/or in the superconductor are not sufficiently small to ensure the strict validity of the dirty limit.<sup>2</sup> On the other hand different authors have performed calculations on supercurrents in such structures when the normal metal is in the clean limit, i.e., when the electron mean free path in *N* is much greater than all the characteristic lengths of the system.<sup>6-9</sup> Unfortunately reported experiments, except perhaps those of Sheperd,<sup>2</sup> have been obtained on systems where the mean

free path (MFP) is not large enough for the metals to be considered in the clean limit.

A description of sample preparation and experimental details are given in Sec. II. In our samples the normal layers are the Sn lamellae of the eutectic and we shall see later that their electronic MFP is always very large; we have therefore analyzed our results assuming that the normal metal is the clean limit.<sup>4</sup> In this way we have obtained good agreement between the experimental variation of the critical current and the theoretical predictions obtained from a combination of Van Gelder's description<sup>10</sup> of the band structure of a periodical *S-N* system and Bardeen and Johnson's calculation of the current in a *S-N-S* contact<sup>9</sup> (Sec. III).

Differential resistances just above the critical current show in certain samples a pronounced increase at temperatures where the critical current itself becomes measurable. This curious effect is also discussed in Sec. III.

In Sec. IV, we discuss our measurements of the critical current as a function of applied magnetic field. The oscillatory dependence of critical current on field is strongly reminiscent of Josephson behavior.

### II. EXPERIMENTAL

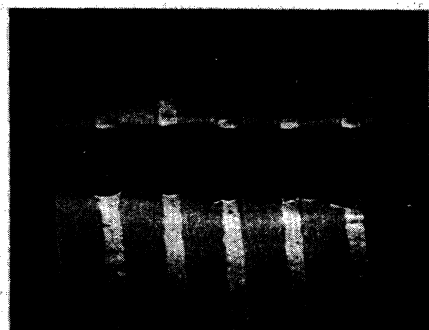
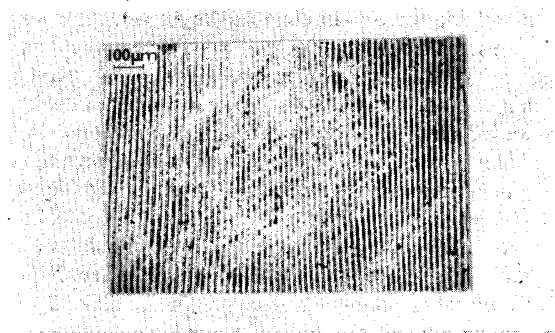
#### A. Samples

Directional solidification of Sn-Pb alloys of eutectic composition<sup>11</sup> can lead to the obtention of nearly perfect lamellar two-phase structure. Each lamella is alternatively a solid solution Pb(Sn) or Sn(Pb) with less than 15 at.% of Sn in the Pb lamellae and 1 at.% of Pb in the Sn lamellae.<sup>12</sup> This lamellar structure is more or less close to ideal depending on the existence of structural faults like terminations or kinks and on the

regularity in the lamellar spacing  $a_E$ .<sup>13</sup>

Pb-Sn eutectic specimens were prepared by melting the appropriate quantities of 99.999 at.% Pb and Sn in an open Pyrex container. Eutectic ribbons were obtained by cold-rolling the rods to a thickness of typically  $25 \mu\text{m}$ . Unidirectional solidification of the ribbons, typically 6 cm long, 2 cm wide, was performed in a flat horizontal furnace.<sup>11,14</sup> The resulting Sn and Pb lamellae are parallel to the direction of growth and perpendicular to the ribbon surfaces; the density of structural faults is relatively low and it is possible to find zones ( $\approx 1 \text{ mm}^2$ ) in which more than 100 lamellae display a perfect structure, the lamellar spacing  $a_E$  being constant ( $\Delta a_E/a_E < 5\%$ ) (Fig. 1). The width of Sn lamellae is  $\frac{2}{3}a_E$ , and that of Pb lamellae is  $\frac{1}{3}a_E$ . Because of capillarity effects  $a_E$  may vary between 2 and  $15 \mu\text{m}$ , depending on the travelling rates of the solidus in the furnace.

Pb lamellae containing a great amount of Sn ( $\approx 15\text{at.}\%$ ) are type-II conductors.<sup>15</sup> Actually, tin has the same valence as lead and becomes a substitutional impurity in it. Rather large concentrations are needed



Eutectic period :  $8 \mu\text{m}$

FIG. 1. Close-to-perfect lamellar structure in the Pb-Sn eutectic alloy and unperturbed structure after cutting of the sample.

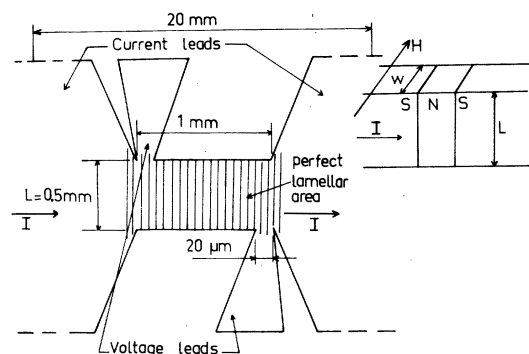


FIG. 2. Schematic view of the sample.

to produce an appreciable reduction of mean free path. On the other hand, tin lamellae contain very little lead and have lattice parameters very close to those of pure-Sn crystals<sup>12</sup>:  $a = 5.830 \text{ \AA}$  and  $c = 3.180 \text{ \AA}$  (Sn eutectic) while  $a = 5.824 \text{ \AA}$  and  $c = 3.175 \text{ \AA}$  (pure Sn). The lamellae are indeed single crystals, very pure and polygonized in the case of Sn while the Pb ones are bent<sup>12</sup>: each Sn subgrain contains 10 to 20 lamellae and is  $250 \mu\text{m}$  long with the lamellar crystals parallel within  $5 \times 10^{-4}$  rad. Further details on sample preparation and properties can be found in Ref. 15.

Regions ( $\approx 1 \text{ mm}^2$ ) of close-to-ideal lamellar structure were located under a microscope and cut away from the remainder of the ribbon. To this end we make use of a microhardness tester with special cutting tool in place of the diamond indenter. The sample was cut along a special pattern (Fig. 3) which provided current and voltage leads; the lamellar structure was checked not to be perturbed by the cutting pro-

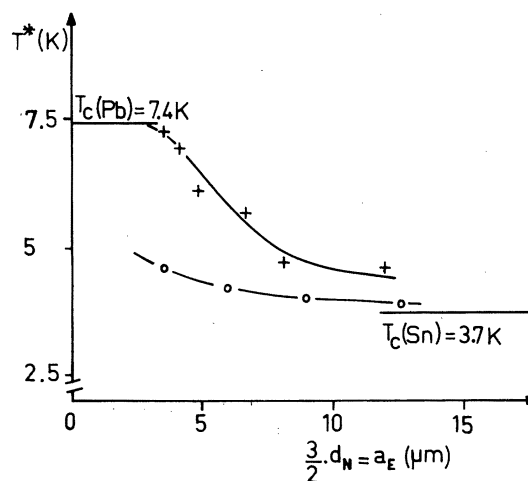


FIG. 3. Variation of  $T^*$  (see text) as a function of lamellar spacing  $a_E$ ; +: our samples, o: single evaporated Pb-Sn junction (Romagnan *et al.*, Ref. 18).

cess (Fig. 1). For a current perpendicular to the lamellae (Fig. 2), we have measured the resistivity  $\rho_{\perp}$  at 8 and 300 K [ $T_c(\text{Pb lamellae}) = 7.4$  K] and therefore we have deduced values of the mean free path  $l$  at 8 K, calculated from Chamber's formula<sup>16</sup> (Table I). The rather large scatter in the  $\rho_{\perp}$  (8 K) values is probably due to interface phenomena (oxide diffusion) since the crystallographic quality of Sn and Pb lamellae remain unchanged from one sample to another. If we introduce the MFP  $l(\text{Sn})$  in the Sn lamellae, the MFP  $l(\text{Pb})$  in the Pb lamellae and the *equivalent* MFP  $l(\text{Sn-Pb})$  which takes into account interface quality, the resulting MFP  $l$  is then given by

$$\frac{1}{l} = \frac{1}{l(\text{Sn})} + \frac{1}{l(\text{Pb})} + \frac{1}{l(\text{Sn-Pb})} \quad (1)$$

Although only a few samples show  $l$  values much greater than the lamellar spacing  $a_E$ , we think that in all samples  $l(\text{Sn})$  is at least equal to the lamella width ( $\frac{2}{3}a_E$ ) and that the  $l$  values smaller than  $a_E$  result from imperfect interfaces through  $l(\text{Sn-Pb})$ .

### B. Measurement techniques

We have determined the resistive transitions of our samples in different magnetic fields and for different temperatures, using conventional cryogenic techniques. A calibrated shunt in series with the sample allows measuring the current with a voltmeter. The system allows a current resolution  $\Delta I/I < 10^{-2}$ . The temperature regulator, of the proportional integral type, uses a germanium thermometer and a differential voltmeter HP 740B, giving a temperature stability better than  $10^{-2}$  K. Because of the very small resistivity of our samples, a current supply must be used for biasing, and voltages are measured with a SQUID (superconducting quantum interference dev-

ice) picovoltmeter with a resolution of  $10^{-12}$  V. Superconducting magnetic shieldings insure that in all cases the residual magnetic fields are smaller than the values of  $H_{c1}$  to be measured.

## III. ELECTRICAL PROPERTIES UNDER ZERO MAGNETIC FIELD

### A. Critical current

We have measured the temperature dependence of the critical current for samples of different lamellar spacing ( $a_E = 4.2, 4.9, 6.7, 8.1, \text{ and } 12 \mu\text{m}$ ). First of all we have determined for each sample a temperature  $T^*$  corresponding to the appearance of a very small supercurrent ( $\approx 10^{-1} \text{ A cm}^{-2}$ ). In Fig. 3, we have plotted  $T^*$  vs  $a_E$ . The value of 7.4 K obtained for the critical temperature of Pb lamellae is greater than the value corresponding to bulk pure Pb (7.2 K). This can be accounted for by the existence of tin in the lead.<sup>17</sup> Romagnan *et al.*<sup>18</sup> have studied evaporated Pb-Sn-Pb junctions in which the width of Sn is 2.4, 4, 6, and 8.4  $\mu\text{m}$  and have determined  $T^*$  using the same definition as ours. The values of  $T^*$  obtained by these authors are also reported in Fig. 2, it can be seen that they are smaller than the values for our eutectic samples; in both cases for large  $a_E$ ,  $T^* \rightarrow T_{c,\text{Sn}}$ , but for small values of  $a_E$ ,  $T^* \rightarrow T_{c,\text{Pb}}$  in our case but not for evaporated junctions. We conclude then that eutectic samples are superior to evaporated ones as regards (i) metallurgical contact between both metals and (ii) purity of the normal metal, Sn in both cases. Therefore proximity effects are stronger in our samples. In previous experiments on bulk eutectic alloys<sup>15</sup> we have already noted that for small lamellar spacings the eutectic behaves like a single superconductor.

Taking into account the very good crystallographic quality of the Sn lamellae we shall calculate the

TABLE I. Principal characteristics of the samples, the temperature behaviors of which are shown in Fig. 4. The junctions may simultaneously be large with respect to the magnetic field ( $L/4\lambda_J > 1$ ; see Ref. 26) and narrow with respect to the current ( $W/4\lambda_J < 1$ ; see Ref. 26). The values of  $\xi_0$  have been obtained by fitting the experimental results with Eq. (11). The mean free path  $l$  has been calculated using Chamber's formula (see Ref. 20) and the value of the normal resistivity at 8 K.

$a_E$ ( $\mu\text{m}$ )	$I_c$ $H=0$ $T=4.2 \text{ K}$ (mA)	$J_c$ $H=0$ $T=4.2 \text{ K}$ ( $\text{A m}^{-2}$ )	$\lambda_J$ $T=4.2 \text{ K}$ ( $\mu\text{m}$ )	$L/4\lambda_J$ $T=4.2 \text{ K}$	$W/4\lambda_J$ $T=4.2 \text{ K}$	$\xi_{0\text{cal}}$ ( $\mu\text{m}$ )	$l$ ( $\mu\text{m}$ )
4.2	50	$1.25 \times 10^7$	2.7	37	0.93	0.40	0.7
4.9	41	$1.28 \times 10^7$	2.5	40	0.80	0.14	600
6.7	29	$7.25 \times 10^6$	3.0	33	0.83	0.25	50
8.1	0.30	$1.04 \times 10^5$	21.0	4	0.10	0.07	0.2
12	4	$5 \times 10^5$	9.0	11	0.22	0.09	4

current in the framework of the theory of Bardeen and Johnson (BJ).<sup>9</sup> These authors assume a superconducting gap in the  $S$  region  $\Delta(s) = \Delta(T=0)$  and in the  $N$  region  $\Delta=0$ , resulting in a quantized quasiparticle spectrum. This is the same approach as that of Kulik<sup>19</sup> and Ishii,<sup>7</sup> but BJ use a simpler mathematical treatment, based on Galilean invariance, to derive the expression of the current. The phase difference across the normal metal is related to the superfluid velocity, and the supercurrent is obtained from the current carrying capacity of quasiparticles in the  $N$  region. The expression found for  $j_c$  is rather complicated, but under the assumption  $T$  not too small, can be approximated by

$$j_c = \frac{6n_e \hbar e}{md_N^*} \exp\left\{\frac{-2d_N^* k_B T}{\xi_0 \Delta(0)}\right\}, \quad (2)$$

with

$$d_N^* = d_N + \pi \xi_0, \quad (3)$$

where  $d_N$  is the width of the normal region,  $m$  and  $e$  are the electron mass and charge, and  $n_e$  is the electronic density.

In fact, the BJ theory has been developed for a single  $S$ - $N$ - $S$  contact, while our samples are series arrays of such junctions. So we must investigate how spatial periodicity can affect the critical current.

The excitation spectrum of a system of alternating regions of lengths  $d_N$  with order parameter  $\Delta=0$  and  $d_S$  with  $\Delta \neq 0$  has been studied by Van Gelder.<sup>10</sup> It consists of a series of allowed and forbidden energy bands. Let the  $S$  and  $N$  regions be along the  $z$  axis, and  $E$  be the energy as measured from the Fermi level. Then, if  $\phi = \sin^{-1}[E/\Delta(T)]$  with  $E < \Delta$ , a convenient expression for the allowed energies is

$$\begin{aligned} \cos[(k_z - k_{zF})a_E] &= e^{A_S \cos \phi} \cos(\phi + A_N \sin \phi) / \cos \phi \\ &+ e^{-A_S \cos \phi} \cos(\phi - A_N \sin \phi) / \cos \phi, \end{aligned} \quad (4)$$

where  $k_z$  is the  $z$  component of the quasimomentum, the period  $a_E = d_S + d_N$ ,  $k_{zF} = (k_x^2 - k_y^2)^{1/2} = k_F |\cos \theta|$ ,  $A_{S,N} = (d_{S,N}/\pi \xi_0 |\cos \theta|) \Delta(T)/\Delta(0)$ .  $\theta$  is the angle between the electron trajectory and the direction of the current.

In our samples  $d_S$  and  $d_N$  are much greater than  $\xi_0$ , so that at not too high temperatures  $A_S \gg 1$ . If, furthermore, we consider energies low enough so that  $\phi \approx \sin \phi = E/\Delta(T)$ ,  $\cos \phi \approx 1$ , expression (4) simplifies considerably, giving

$$\begin{aligned} \cos[(A_N + 1)E/\Delta] &= (-1)^n \sin[(A_N + 1)E/\Delta - (n + \frac{1}{2})\pi] \\ &\approx e^{-A_S} \cos ka \ll 1. \end{aligned} \quad (5)$$

The allowed energies are then defined by

$$|E - E_n| \leq \Delta e^{-A_S}/(A_N + 1), \quad (6)$$

with

$$E_n = (n + \frac{1}{2})\pi \Delta(T)/(A_N + 1). \quad (7)$$

The bands are then seen to become extremely narrow as  $T$  decreases and hence  $A_S$  increases. This is shown in Fig. 4 where a numerical solution of Eq. (4) is plotted. It is also seen that expressions (6) and (7) are valid even when  $E \approx \Delta$ . Now, Eq. (7) is just the expression for the energy levels in the  $N$  region of a single  $S$ - $N$ - $S$  junction as obtained by Bardeen and Johnson provided  $\Delta(S)$  is replaced by  $\Delta(T)$ . (This is not surprising since in the latter, as well as in Van Gelder's work on multiple contacts, Bogoliubov equations are solved with a square gap parameter well.) The levels are those of an infinite potential well with an effective width

$$d_N^* = d_N + \pi \xi_0 |\cos \theta| \Delta(0)/\Delta(T). \quad (8)$$

Proceeding now to a calculation of the current which exactly parallels that of Bardeen and Johnson,<sup>9</sup> we find for the maximum supercurrent:

$$j_c = \frac{6n_e \hbar e}{md_N} \exp\{-2[d_N + \pi \xi_0 \Delta(0)/\Delta(T)]k_B T/\xi_0 \Delta(0)\}. \quad (9)$$

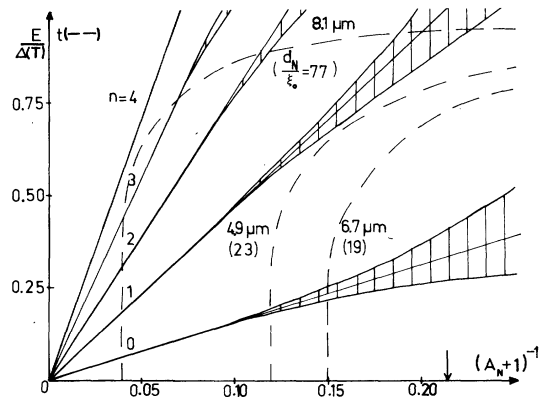


FIG. 4. Band structure of a periodical  $S$ - $N$  system according to Eq. (4) in the text with  $A_S = \frac{1}{2}A_N$ . Hatched regions correspond to allowed energy bands. The straight lines passing through the origin represent low-lying quasiparticle levels of a single  $SNS$  junction given by Eq. (7). Band structure of actual samples can be related to reduced temperature  $t = T/T_{c, PB}$  through the dashed lines. They are solutions of Eqs. (13) and (14) in the text. For a given value of  $t$  they give  $(A_{N+1})^{-1}$  with  $\cos \theta = 1$ , i.e., for forward moving electrons. The arrow marks the value of  $(A_{N+1})^{-1}$  for which the  $n=1$  level is fully inside the well.

Equation (9) is equivalent to (2) provided the effective normal length (3) is replaced by

$$d_N^* = d_N + \pi \xi_0 \Delta(0) / \Delta(T) \quad (3')$$

which is a natural consequence of having introduced the temperature dependence of the gap parameter potential well. A further replacement is that of  $d_N^*$  in the preexponential term of Eq. (2) by  $d_N$  in Eq. (9). This amounts to only a few percent difference unless  $T$  is in the immediate vicinity of  $T_{c\text{pb}}$ .

We emphasize again that this calculation is only valid in the temperature range where the width of the band is very small compared with  $k_B T$ . This temperature range can be estimated from the plots in Fig. 4.

We use the expression given by Thouless<sup>20</sup> for the temperature dependence of the gap parameter of a strong coupling superconductor:

$$\delta = \Delta(T) / \Delta(0) = \tanh(\delta/t) \quad (10)$$

where  $t = T/T_c$ .

In lead  $\Delta(0) \approx 2k_B T_c$ , so that Eq. (9) leads to

$$j_c = \frac{6n_c \hbar e}{md_N} \exp\{-[4a_E \tanh(\delta/t) / 3\xi_0 + \pi]t/\delta\} \quad (11)$$

We have compared this expression with our experimental results obtaining least-squares fits with  $\xi_0$  and the preexponential term as adjustable parameters. The fits are shown in Fig. 5 together with the data. In all cases the critical current density has been calculated from the critical current assuming narrow junctions. This is consistent with the values of the Josephson penetration depth shown in Table I. The values of  $\xi_0$  giving the best fits are given in Table I. They correspond roughly to what can be expected for lead (0.1 to 0.2  $\mu\text{m}$ ), particularly for samples having the greatest lamellar periods. This is to be related to another fact, namely, that the fits become poorer at high temperatures for samples having  $T^*$  sufficiently close to  $T_{c\text{pb}}$ , i.e. those with the shortest periods. There are two reasons for that: firstly, the value of  $\Delta(T)$  obtained from Eq. (9) is that of bulk material, while the potential well should be rather defined by  $\Delta_I(T)$ , the order parameter at the interface.

Since on the normal side  $\Delta$  changes on a length scale  $\sim \xi_0$ , while in the superconductor it requires a length  $\xi(T)$ ,  $\Delta_I(T) \approx \Delta(T) \xi_0 / \xi(T)$ , i.e.,  $\Delta_I(T) \ll \Delta(T)$  when  $T \approx T_c$ . Secondly, the thinner (shorter period) and shallower (higher temperature) is a potential well, the smaller the number of levels it can accommodate. Thus the contribution to the current of the continuous spectrum, not taken into account in the above calculation, becomes relatively more important at high temperature.<sup>9</sup>

Nevertheless in order to check further the consistency of our results, we have plotted in Fig. 6 the

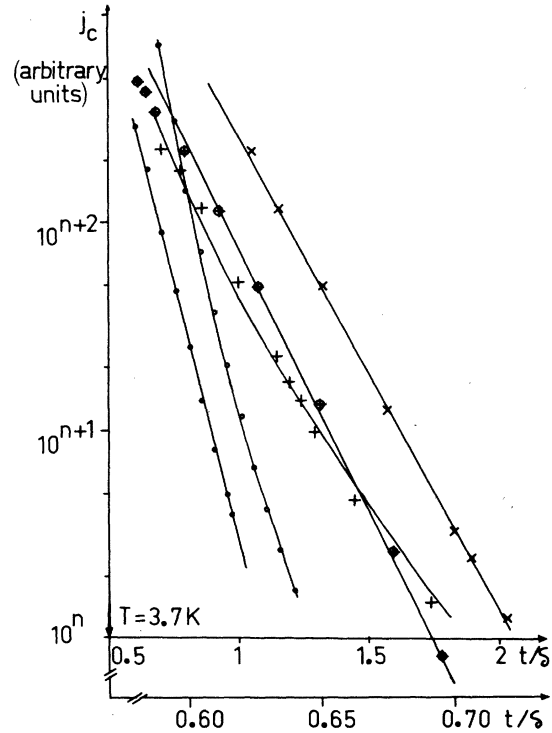


FIG. 5. Critical current  $j_c$  vs the reduced variable  $t/\delta = t\Delta_{\text{BCS}}(0)/\Delta_{\text{BCS}}(t)$  for various samples of different lamellar spacings  $a_E$ . Experimental data: +:  $a_E = 12 \mu\text{m}$ ; x:  $a_E = 8.1 \mu\text{m}$ ; •:  $a_E = 6.7 \mu\text{m}$ ; o:  $a_E = 4.9 \mu\text{m}$ ; •:  $a_E = 4.2 \mu\text{m}$ . The data corresponding to  $a_E = 12$  and  $8.1 \mu\text{m}$  refer to the lower  $t/\delta$  scale, with a corresponding shift of the  $j_c$  scale. The solid lines are the theoretical curves obtained by the fitting procedure described in the text.

logarithmic variation of  $a_E j_c$  vs  $a_E$  at  $T = 4.22 \text{ K}$ . According to Eq. (11) with the proper values of  $t = 0.57$  and  $\delta/t = 0.62$ , and an average value of  $\xi_0$ ,  $\xi_0 = 0.15 \mu\text{m}$ , as given by the preceding analysis:

$$a_E j_c \propto \exp(-2.5a_E) \quad (12)$$

The exponential dependence on  $a_E$  is well verified. However, slightly different slopes are found depending on sample resistivity ( $-0.4 \mu\text{m}^{-1}$  for samples of very low resistivity,  $-0.6 \mu\text{m}^{-1}$  for those of higher resistivity). An equivalent MFP making no distinction between volume and interface collisions, may be calculated from the resistivities. If this is then compared with the period, the two slopes shown in Fig. 6 correspond roughly to samples (i) where electrons are almost certain to traverse a few periods without collisions and (ii) where they suffer more than one collision per period. The discrepancy between experimental slopes and those predicted by Eq. (12) is apparently in contradiction with the rather good agreement

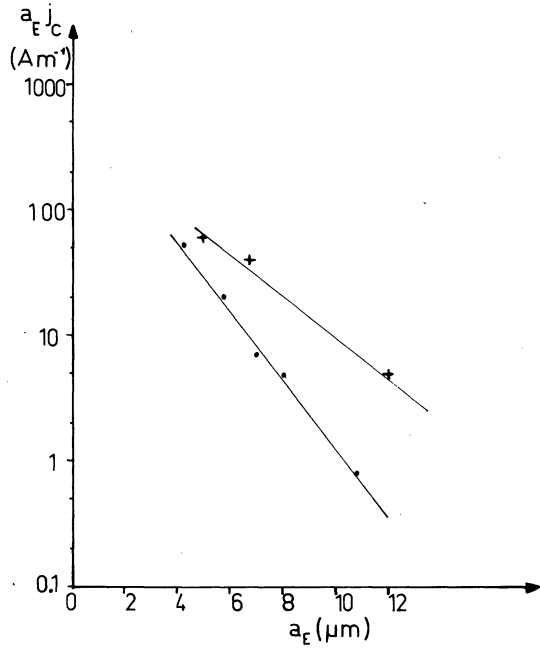


FIG. 6. Product  $a_E j_c$  vs lamellar spacing  $a_E$  at a given temperature ( $T = 4.2$  K). +: samples of very low normal resistivity ( $\rho < 10^{-10}$   $\Omega$  m); o: samples of high normal resistivity ( $\rho \approx 10^{-9}$   $\Omega$  m).

obtained between Eq. (11) and experiment. In fact, Eq. (11) has been derived for ideally clean samples, and its comparison with experiment concerns only the exponential term. On the other hand, Eq. (12) assumes that the preexponential factor is independent of MFP in the normal metal, which is probably not true.

We have also measured the variation of  $j_c$  vs  $T$  for temperatures smaller than  $T_{c,Sn} = 3.7$  K; in that regime the eutectic alloy is an  $S$ - $S'$ - $S$  system, the superconductivity of  $S'$  (Sn lamellae) being weaker than that of  $S$  (Pb lamellae). A typical  $I_c(T)$  curve is represented on Fig. 7 for a sample of lamellar spacing  $a_E = 12$   $\mu$ m. Apart from an anomaly around  $T = 3.7$  K, probably due to the thermodynamical superconducting transition of the Sn lamellae, it appears that in the low temperature range  $I_c$  varies linearly with  $T$ ; the high temperature range corresponds to the figure 5. This linear dependence differs from the results obtained by Romagnan *et al.*<sup>21</sup> whose samples behave like a bulk superconductor,  $j_c = j_0(1 - t')^{3/2}$  ( $t' = T/T_{c,Sn}$ ). Thus it seems that our samples still present a Josephson-like behavior for  $T < 3.7$  K, the linear variation of  $I_c$  could then be accounted for by a model of coherent vortex motion in  $S'$  similar to that proposed by Likharev.<sup>22</sup> Indeed Adde *et al.*<sup>23</sup> have also observed a linear dependence of  $I_c$  vs  $T$  for Dayem bridges obtained by ion-beam etching, the critical temperature of the bridge being smaller than that of the superconducting electrodes.

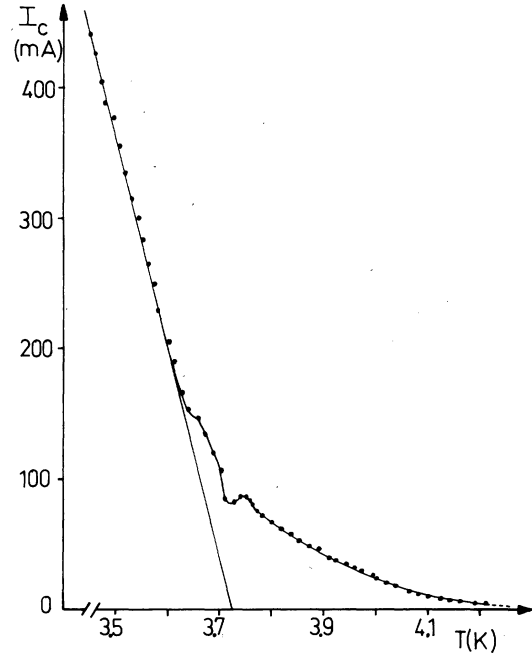


FIG. 7. Typical  $I_c(T)$  curve showing anomalous behavior near the critical temperature of tin ( $T_{c,Sn} = 3.7$  K).

#### B. $V(I)$ characteristics and differential resistivity

The  $V(I)$  characteristic of a typical sample is shown in Fig. 8. It shows a linear region [ $V = R_D(I - I_c)$ ] in a current interval at least of the order of the critical current itself. The resulting differential resistivity  $\rho_1$  in this region is plotted as a function of reduced temperature in Fig. 9 for several samples. A striking fact appears: samples with a rather high normal resistivity display a  $\rho_1(T)$  steadily decreasing below  $T_c(Pb)$ , while those having the lowest normal resistivity show a sudden increase in  $\rho_1$ , at  $T \approx T^*$  (three orders of magnitude in the case of the  $a_E = 4.9$   $\mu$ m sample) where the critical current becomes measurable. The first type of behavior has been observed in single  $S$ - $N$ - $S$  contacts<sup>24,25</sup> and explained as due to charge build-up in the  $N$ - $S$  interfaces. It should be particularly noticeable under heavy interface scattering.<sup>24</sup>

On the other hand, it is well known that an ideal Josephson device should present a singularity in dynamical resistance at  $I = I_c$ . However, the rather large current interval over which the dynamical resistance is practically constant precludes such an interpretation in our case. Furthermore although for many samples  $T^*$  is only related to the sensitivity of our apparatus, in the case of very low resistivity ones (cf. Fig. 9) a few experimental points hint to a sudden decrease of supercurrent at temperatures above  $T^*$ . The coincidence of the two phenomena (supercurrent and resistivity decrease with increasing temperatures)

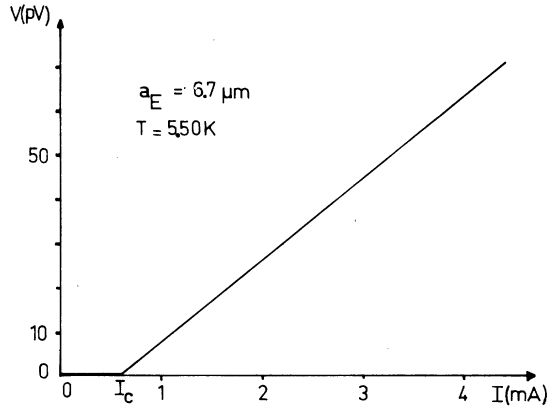


FIG. 8. Typical resistive  $V(I)$  characteristic showing the linear behavior above  $I_c$ .

suggests that in such cases  $T^*$  may have a deeper than purely instrumental physical meaning. To avoid any confusion in what follows we shall keep  $T^*$  applying to an instrumental threshold and let  $T_1$  mark a sudden change in supercurrent and resistivity. We suggest here that both phenomena are related to the appearance of the  $n = 1$  bound level on top of the pair potential well.

Let us consider the creation of new bound levels as the potential well grows deeper with decreasing tem-

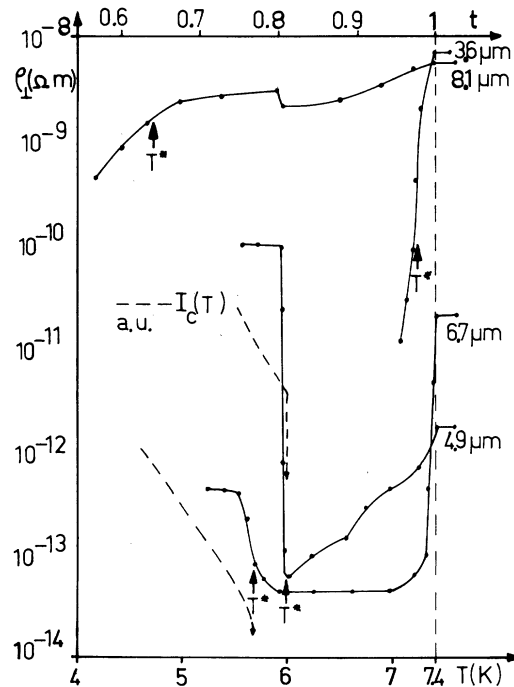


FIG. 9. Differential resistivities  $\rho_{\perp}$  and critical currents  $I_c$  as function of reduced temperature.

perature. The position of the level (or middle of the band) is found by equating to zero the right-hand side of Eq. (4). By requiring then that  $E/\Delta(T) = \sin\phi \rightarrow 1$  and taking into account that in our samples  $A_S = \frac{1}{2}A_N$ , one finds the  $n = 1, 2, 3, \dots$  level on the top of the well whenever  $A_N$  is a solution of the transcendental equation  $A_N \tan A_N = 2$ . The first solution ( $n = 1$ ) is found to be  $A_N = 1.16\pi$ . Electrons moving normal to the lamellae ( $|\cos\theta| = 1$ ), with energy  $E_1$ , will then be sitting on top of the well when

$$\delta_I(t) = \Delta_I(T)/\Delta(0) = 1.16\pi^2\xi_0/d_N. \quad (13)$$

Now

$$\Delta_I(T) = \Delta(T)\xi_0/\xi(T) \approx \Delta^2(T)/\Delta(0), \quad (14)$$

where the last step follows from the qualitatively correct assumption that  $\xi(T) \propto \Delta^{-1}(T)$  over the whole temperature range. Therefore  $\delta_I(t) = \delta^2(t)$  and one can solve Eq. (13) for  $t$  for each sample. This is, on the one hand, the temperature at which quasiparticles in the  $n = 1$  level have not enough energy to overcome the potential barrier when the phase difference is zero. On the other hand, actually the energy depends on phase difference  $\pi\gamma$  as<sup>19</sup>:

$$E_n \approx \frac{\hbar v_F |\cos\theta|}{d_N'^*} \pi \left[ n + \frac{1}{2}(1 \pm \gamma) \right]. \quad (15)$$

This is also very closely the temperature at which  $n = 0$  electrons remain in the well during a whole phase sweep. It is only at this temperature that the discrete spectrum can start contributing efficiently to the supercurrent, and this would explain its sharp increase. We find, using the  $\xi_0$  values obtained from fitting the  $I_c(T)$  curves (Table I),

$$t_1 = 0.807 \quad (a_E = 4.9 \mu\text{m}) \quad \text{and} \quad t_1 = 0.728 \quad (a_E = 6.7 \mu\text{m})$$

The corresponding experimental values are  $0.81 \pm 0.02$  and  $0.76 \pm 0.02$ . This rather good agreement is probably only fortuitous because of the approximate character of expression (14).

The increase of resistivity below  $T_1$  at  $I \geq I_c$  can be understood, at least qualitatively, through a similar argument. First of all, let us point out that the measured resistivity at the minimum of the  $\rho_{\perp}(T)$  curve for our cleanest samples ( $a_E = 4.9$  and  $6.7 \mu\text{m}$ ) is of the order of magnitude of what can be expected for tin ( $\approx 10^{-11} \Omega \text{cm}$ ) on the basis of the Bloch-Grüneisen formula for the ideal resistivity of metals at helium temperatures. We can then assume that  $\rho_{\perp}(T)$  is mostly due to the electron-phonon interaction. Let us now consider what happens when  $I_c \neq 0$ . As the current increases above  $I_c$ , the phase difference across a normal region is forced to oscillate between  $-\pi$  and  $\pi$ . This brings about an oscillation of the whole discrete spectrum, which sweeps over the potential well,<sup>19</sup> its structure remaining otherwise un-

changed. On the other hand, the average contribution of the continuous spectrum to the total current increases as the current carrying capacity of the quantized levels saturates. Excitations in the continuum give up their excess energy by phonon emission. Above  $T_1$ , there is a single level [ $n=0$  in Eq. (15)] in the well. Electron-phonon transitions can then occur between states in the continuum or between the continuum and this level. Now, the existence of an intermediate level is known to greatly enhance emission and absorption probabilities, and therefore the phonon induced resistance. This is what happens at  $T < T_1$ , as the  $n=1$  level is formed. The analogy between this description and that of a three-level laser should be noted, phonons replacing photons in our case. One should expect that the whole effect would be more marked the narrower the levels. If this is correct, the  $\rho_1$  increase shown by the  $a_E = 4.9 \mu\text{m}$  sample, much more important than that of the  $a_E = 6.7 \mu\text{m}$  one, would be related to the narrower bands (see Fig. 4) of the former at  $T_1$ .

We point out that a certain number of conditions have to be satisfied for this effect to become observable. First of all, exceptionally clean samples are required so that collisions with impurities should not mask the phonon resistance. The temperature  $T_1$ , defined by Eq. (13) should be such that  $k_B T_1 \ll E_1 - E_0$  (for a measurable current to exist), and the bandwidth  $\delta E \ll E_1 - E_0$ . This implies that  $d_N$  be not too large, since in such a case  $T_1 \rightarrow T_c$ . The current given by Eq. (11) may then be too small to be measured at this temperature. The experimental value of  $T^*$  (and not  $T_1$ ), will be defined only by the threshold sensitivity of the apparatus. On the other hand, a very small  $d_N$  means that the well will contain a single level down to  $T=0$  and therefore the supercurrent observed is mainly due to contributions from the continuous spectrum and/or the proximity effect.

#### IV. INFLUENCE OF THE MAGNETIC FIELD

One of the most typical features of the Josephson effect in  $S$ - $I$ - $S$  junctions, is the well-known Fraunhofer pattern of the critical current versus magnetic field,  $j_c(H)$ , curves. However this behavior appears only when the junction is narrow, i.e., the dimension  $L$  perpendicular to the field is smaller than the Josephson penetration depth  $\lambda_J$ ; in contrast large junctions ( $L \gg \lambda_J$ ) exhibit a Meissner effect at low applied magnetic fields<sup>26</sup> and then a complex vortex structure<sup>27</sup> with overlapping magnetic modes. For  $S$ - $N$ - $S$  structures the values of  $\lambda_J$  are generally much smaller than in  $S$ - $I$ - $S$  junctions, so in most cases the former behave like large junctions ( $L \gg \lambda_J$ ) exhibiting an irregular modulation of  $j_c$  vs  $H$ , the critical current never reaching a zero value.<sup>28</sup> Our samples show such a behavior, thereby indicating that, in spite

of the large thicknesses of normal metal involved, Pb-Sn lamellar eutectic actually show a Josephson-like effect. The measurements of  $I_c(H)$  have demonstrated the existence of hysteretic effects, probably due to pinned vortices in the junction; Therefore to obtain the experimental curves we have always driven the samples normal, heating them, between two measurements at different values of  $H$  so as to avoid pinning effects. On Fig. 10 are reported the experimental  $I_c(H)$  curves at two temperatures ( $T=4.40$  and  $4.55$  K) for the sample of lamellar spacing  $a_E = 12 \mu\text{m}$  for which  $T^* = 4.65$  K. At these temperatures the calculated values of  $L/\lambda_J$  being, respectively, 38 and 22, the junctions are actually in the very large limit for magnetic field penetration. The modulation of  $I_c(H)$  appears on the two curves but is more pronounced at  $T=4.55$  K; this is actually a general feature of our experiments: the modulation of  $I_c(H)$  is deeper the closer  $T$  is to  $T^*$ . It is also noteworthy that the pseudoperiod  $\Delta H$  of the modulation decreases as  $T$  approaches  $T^*$ , so for the preceding sample one can approximately determine  $\Delta H \approx 0.5$  Oe at 4.40 K and  $\Delta H \approx 0.2$  Oe at 4.55 K. We think that this decrease of  $\Delta H$  is related to a variation of the effective thickness of the normal region rather than to a variation of the penetration depth in lead, which is nearly a constant in this temperature range; this modification of the normal thickness could be accounted for in BJ's model by the alteration of  $d_N^*$  with temperature [cf. Eq. (3')]. We have also carried out some measurements of  $I_c(H)$  at temperatures lower than the critical temperature of tin ( $T < T_{c\text{Sn}}$ ); in this temperature range the results are not so clear. For instance for the sample of  $a_E = 12 \mu\text{m}$ , the  $I_c(H)$  curve at  $T=3.55$  K is shown in Fig. 10(a): critical current modulation appears only at relatively high values of  $H$ . A possible explanation of this phenomenon would be the following: the thickness of tin  $d_N = \frac{2}{3}a_E = 8 \mu\text{m}$  is greater than the spatial extent of Josephson vortices so at small applied fields coherent motion of vortices can hardly occur, but coherent motion can take place when a sufficient number of vortices enter the contact by increasing  $H$ .

From the curves  $I_c(H)$ , it is also possible to determine  $H_{c1}$ , the maximum field at which the Meissner solution exists in the junction. The features of the  $I_c(H)$  curves make this determination only approximate, however it may be interesting to carry out a comparison between the experimental and the theoretical values of  $H_{c1}$  for samples having different lamellar spacings. The theoretical value of  $H_{c1}$  is given by<sup>26</sup>:

$$H_{c1} = \phi_0 / \pi \lambda_J (2\lambda + d_N) \quad (16)$$

where  $\lambda_J = [\hbar c^2 / 8 \pi e j_c (2\lambda + d_N)]^{1/2}$  is the Josephson penetration depth,  $\lambda$  is the penetration depth in the lead, and  $d_N$  is the thickness of the normal region (the Sn lamellae); for our samples  $d_N = \frac{2}{3}a_E$ . In order to

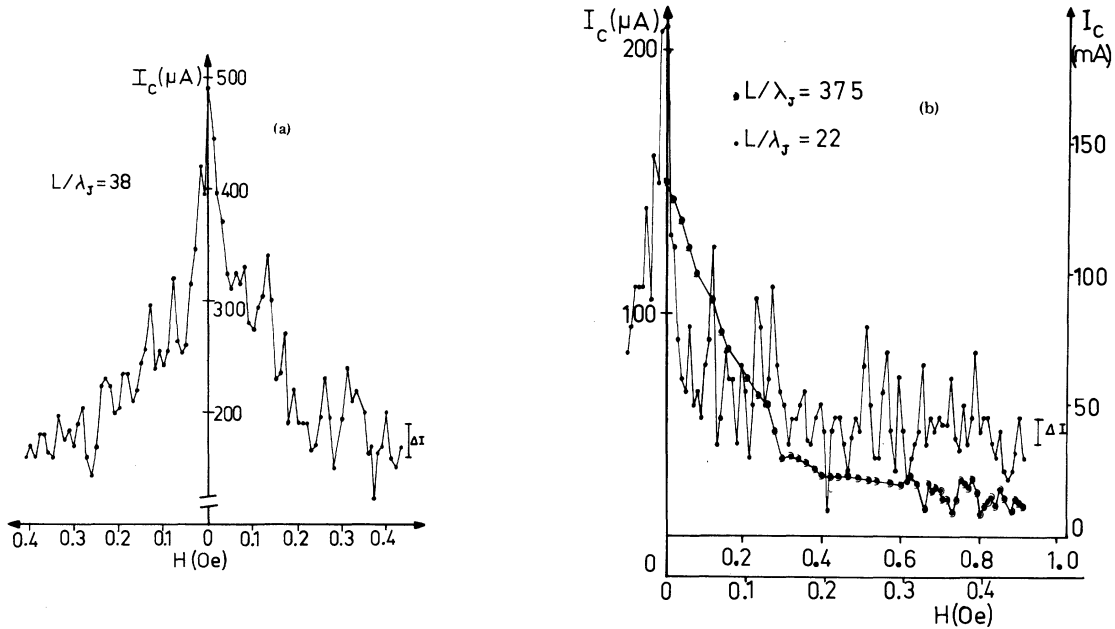


FIG. 10. Critical current as a function of applied magnetic field  $I_c(H)$  at a given temperature for a sample of  $a_E = 12 \mu\text{m}$ : (a)  $T = 4.40 \text{ K}$ . The residual magnetic field has been subtracted and the curve appears to be nearly symmetrical. (b)  $\bullet$ :  $T = 4.55 \text{ K}$ , this curve is referred to the left  $I_c$  scale and to the lower  $H$  scale;  $\bullet$ :  $T = 3.55 \text{ K}$  (below the critical temperature of tin,  $T_{c\text{Sn}} = 3.7 \text{ K}$ ), this curve is referred to the right  $I_c$  scale and to the higher  $H$  scale. The residual magnetic field has been subtracted in both cases.

calculate  $\lambda_J$  we must assume that the junction is either narrow or large with respect to the current. Then we check the result by comparing the calculated value of  $\lambda_J$  with  $\frac{1}{4}w$ .<sup>26</sup> So in our case we can consider that the current flows uniformly in the samples. In Fig. 11 we have plotted  $H_{c1}$  as a function of the lamellar spacing  $a_E$  at the temperature  $T = 4.2 \text{ K}$ . Keeping in mind the uncertainties involved in the experimental values of the critical fields and of  $\lambda_J$  we can conclude that the agreement between the calculated and the measured

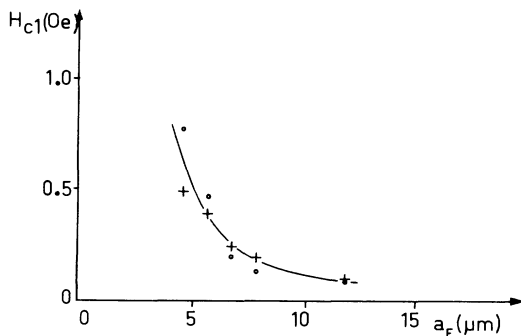


FIG. 11. Calculated and measured values of  $H_{c1}$  vs lamellar spacing: +: experimental; o: calculated from Eq. (16). The full line is only a guide for the eye.

values is rather satisfactory. As a function of the temperature, we have observed a rapid decrease of  $H_{c1}$  near  $T^*$ , which can probably be related to the same mechanism as the above-mentioned decrease of  $\Delta H$ .

## V. DISCUSSION

Our experiments show that lamellar eutectic systems can provide relevant information on the superconducting properties of  $S-N-S$  contacts in a domain hardly attained by other procedures, namely, that of very clean materials in exceptionally good metallurgical contact. The temperature dependence of the critical current confirms theoretical predictions which assume that the main contribution to the current comes from discrete quasiparticle levels in the normal metal, at least when the number of these levels is high ( $d_N \gg \xi_0$ ). Possible deviations from this rule may be expected when only a few bound levels are allowed in the well. This may be the reason for the abnormally high values of  $\xi_0$  fitting the experimental results on samples with the shortest periods (see Table I). However, in the absence of detailed calculations in this case, this remains an open problem. Another open question is the modification of supercurrents due to bulk and/or interface scattering, i.e., the intermediate region

between the dirty (proximity effect) and clean (quantized levels) limits. Our results suggest that mean free path effects appear mainly in the temperature-independent preexponential term in the expression for the supercurrent. This may also be the origin of the systematic discrepancy that we find between theoretical values of this factor and those resulting from our experiments. The latter are about two orders of magnitude smaller than predicted values. A similar discrepancy has been observed by Shepherd<sup>2</sup> when comparing his results with de Gennes proximity effect theory.<sup>5</sup>

Exceptionally clean samples of intermediate lamellar periods show a sudden increase both in supercurrent

and dynamical resistance at  $I > I_c$  at a certain temperature. This curious effect and the tentative interpretation we have given of it emphasize the role that phonons together with quasiparticles level quantization may play in these systems.

Finally the influence of the magnetic field supports well the Josephson behavior of our eutectic structures at least in the temperature range between  $T_{cN}$  and  $T_{cS}$ . For temperatures below  $T_{cN}$  the situation is not so clear. Indeed, the modulation of the critical current for high values of  $H$  is not sufficient to completely discard a bulk type behavior of the current, the more so that it is rather difficult to distinguish experimentally a linear temperature dependence from a  $\frac{3}{2}$  power law.

\*Supported in part by Direction des Recherches et Moyens d'Essai du Ministère de la Défense Nationale (DRME) and Recherche Coopérative sur Programme (RCP) 235 of the Centre National de la Recherche Scientifique (CNRS).

<sup>†</sup>Also Institut National de Sciences Appliquées, 35031-RENNES.

<sup>‡</sup>Associated to CNRS.

<sup>1</sup>J. Clark, Proc. R. Soc. A **308**, 447 (1969).

<sup>2</sup>J. G. Shepherd, Proc. R. Soc. A **326**, 421 (1972).

<sup>3</sup>D. W. Palmer and J. E. Mercereau, Appl. Phys. Lett. **25**, 467 (1974).

<sup>4</sup>J. M. Dupart and J. Baixeras, Appl. Phys. Lett. **30**, 123 (1977).

<sup>5</sup>P. G. de Gennes, Rev. Mod. Phys. **36**, 225 (1964).

<sup>6</sup>I. O. Kulik, Zh. Eksp. Teor. Fiz. **57**, 1745 (1969) [Sov. Phys.-JETP **30**, 944 (1970)].

<sup>7</sup>C. Ishii, Prog. Theor. Phys. **44**, 1525 (1970).

<sup>8</sup>A. V. Svidzinskii, T. N. Antsygina, and E. N. Bratus, Zh. Eksp. Teor. Fiz. **61**, 1612 (1971) [Sov. Phys.-JETP **34**, 860 (1972)].

<sup>9</sup>J. Bardeen and J. L. Johnson, Phys. Rev. B **5**, 72 (1972).

<sup>10</sup>A. P. Van Gelder, Phys. Rev. **181**, 787 (1969).

<sup>11</sup>R. Racek, Thèse de doctorat ès Sciences physiques (Nancy I, 1973) (unpublished).

<sup>12</sup>B. Labulle and C. Petipas, J. Cryst. Growth **28**, 879 (1975).

<sup>13</sup>A. Guinier, C. Petipas, G. Sauvage, J. Baixeras, J. M. Dupart, G. Fournet, G. Fontaine, M. G. Blanchin, M. Turpin, and R. Racek, *Conference on In Situ Composites—Lakeville, Conn.* (National Material Advisory Board, Washington

D.C., 1973), Vol. III, p. 85.

<sup>14</sup>J. J. Favier, Thèse de docteur-ingénieur (Grenoble, 1976) (unpublished).

<sup>15</sup>J. M. Dupart, R. A. Brand, J. Baixeras, and O. Bethoux, J. Phys. **38**, 393 (1977).

<sup>16</sup>R. G. Chambers, Proc. R. Soc. A **215**, 481 (1952).

<sup>17</sup>E. Nembach, J. Phys. Chem. Solids **29**, 1205 (1968).

<sup>18</sup>J. P. Romagnan, A. Gilabert, J. P. Laheurte, J. C. Noiray, and E. Guyon, Solid State Commun. **16**, 359 (1975).

<sup>19</sup>I. O. Kulik, Zh. Eksp. Teor. Fiz. **57**, 941 (1969) [Sov. Phys.-JETP **30**, 944 (1970)].

<sup>20</sup>D. J. Thouless, Phys. Rev. **117**, 1256 (1960).

<sup>21</sup>J. P. Romagnan, A. Gilabert, J. C. Noiray, E. Guyon, Solid State Commun. **14**, 83 (1974).

<sup>22</sup>K. K. Likharev, Zh. Eksp. Teor. Fiz. **61**, 1700 (1971) [Sov. Phys.-JETP **34**, 906 (1972)].

<sup>23</sup>R. Adde, P. Crozat, S. Gourrier, G. Vernet, M. Bernheim, and D. Zenatti, Rev. Phys. Appl. **8**, 455 (1973); **9**, 181 (1974).

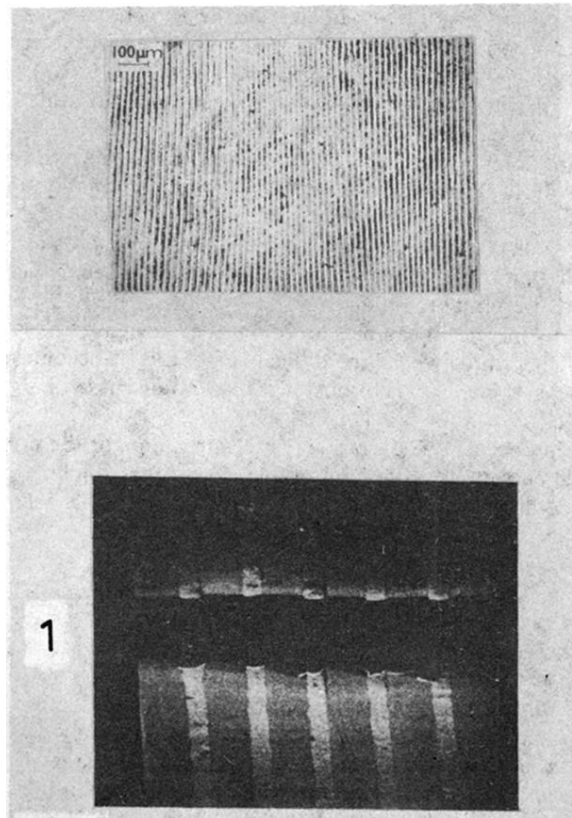
<sup>24</sup>A. B. Pippard, J. G. Shepherd, and D. A. Tindall, Proc. R. Soc. A **324**, 17 (1971).

<sup>25</sup>G. L. Harding, A. B. Pippard, and J. R. Tomlinson, Proc. R. Soc. A **340**, 1 (1974).

<sup>26</sup>R. A. Ferrel and R. E. Prange, Phys. Rev. Lett. **10**, 479 (1963).

<sup>27</sup>C. S. Owen and D. J. Scalapino, Phys. Rev. **164**, 538 (1967).

<sup>28</sup>A. M. Goldman and P. J. Kreisman, Phys. Rev. **164**, 544 (1967).



Eutectic period :  $8 \mu\text{m}$

FIG. 1. Close-to-perfect lamellar structure in the Pb-Sn eutectic alloy and unperturbed structure after cutting of the sample.